On the Potentialities of Reduced Structure Inverter Integrated in Robot Application

Lilia Zouari, Asma Ben Rhouma and Mohamed Abid

***Abstract*—This paper proposes an approach to improve the cost-effectiveness of the control of variable speed drives in the robotics field. This could be achieved by the association of brushless DC motors (BLDCM)with a reduced structure DC/AC converter that is the three-switch inverter (TSI) equipping a robot arm. In a first step, we devoted the analysis, modelisation and control of a three-switch inverter (TSI), also known delta-inverter, fed BLDCM drive. A special attention is paid to the implementation of a dedicated strategy in such a drive and the comparison of its performance with those given by the conventional inverter fed BLDCM drive. A dynamic model and the control of a robot arm have been developed. Finally, simulation results carried out in Matlab-Simulink environment considering the association of both conventional and reduced inverter fed BLDCM drive with a robot arm are treated.**

***Index Terms*—BLDCM, control, robot arm, simulation, three-Switch Three-Phase Inverter (TSTPI).**

I. Introduction

THE brushless DC machines (BLDCM) have been gaining a lot of interest over the last few years. Such an increasing attention is due to several advantages including the absence of brushes which provide robustness, reliability and simplicity of its implementations [1], [2], [3], [4].

For this reason, the BLDCM is considered an interesting candidate in the variable speed applications, especially the robotic one [5], [6], [7], [8], [9], [10].

Therefore, the total cost of a variable speed system is dominated by the cost of the controller.

Currently, an increasing attention is given to improve the cost-effectiveness and the compactness of the machine drives representing the actuators of the robot arm as well as the reduction of the execution time of the control algorithm which represent crucial cost benefits especially for robotic applications.

Thanks to the significant advances in the power electronic converters, the cost-effectiveness and the reliability of electric machine drive can be established by reducing structure of the associated converter.

Within this trend, a novel inverter topology the so-called "Three-Switch Three-Phase Delta-shaped Inverter (TSTPI)" is presented. It allows a reduction of the number of the power switches from six in the conventional six-switch three-phase inverter (SSTPI) to three.

In one previous work [11], the analysis and control of TSTPI fed brushless DC motors for propulsion application have emphasized the drive high performance, whose comparison with the one yielded by six-switch three-phase inverter (SSTPI) fed BLDCM drives has reveled almost the same behavior with a 50 % reduction of the inverter's structure.

Within the same approach, the paper is devoted to improve the cost-effectiveness, the compactness and the reliability of the control of TSTPI fed brushless DC motors for robotic applications.

Manuscript received March 20, 2012; revised April 03, 2012.

L.Zouari and M.Abid are with the laboratory on Computer and Embedded Systems(CES), A.B Rhouma is with the Research Unit on Renewable Energies and Electric Vehicles(RELEV), Department of Electrical Engineering, National School of Engineering of Sfax, Tunisia, Sfax University. e-mail:lilia6enis@yahoo.fr; asma.benrhouma@yahoo.fr; mohamed.abid@enis.rnu.tn.

II. Basis of TSTPI Fed BLDCM Drives

Figure 1 shows the topology of the TSTP delta-shaped inverter (TSTPI). Each leg of the inverter includes the third of the battery pack in series with a set made up of an IGBT and an antiparallel-connected diode. The so-arranged legs are delta-connected and their summits feed the BLDCM.

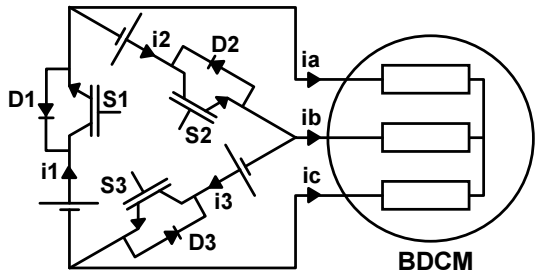

Fig. 1. TSTPI fed BLDCM Drive Connections

In the case where the machine generates trapezoidal back EMFs, it should be fed by 120 electrical-degree rectangular currents in order to achieve high torque with reduced ripples. It is to be noted that the operation of the BLDCM can be divided into six different operating sequences with in each just two phases are fed.

The six operating sequences of the BLDCM with a TSTPI in the armature are achieved as shown in figure 2, where thick lines indicate the conducting circuits. Both active subsequences (during which the motor is fed through IGBT(s)) and regenerative subsequences (where the motor is connected to the DC bus through diode(s)), yielded by bang-bang current regulation of the IGBTs, are illustrated.

A characterization of the six operating sequences of the BLDCM is summarized in table I.

III. Dedicated Control Strategy

The present section deals with the implementation of a dedicated self strategy in the TSTPI-fed BLDCM drive. Basically, it consists of an *abc*-control strategy, where the self-control angle ψ is kept null, so that the electromagnetic torque turns to be maximum:

$$T_{em}^{\psi=0} = 3p\ \Phi_{pm} I_a \quad (1)$$

ISBN: 978-988-19252-1-3
ISSN: 2078-0958 (Print); ISSN: 2078-0966 (Online)

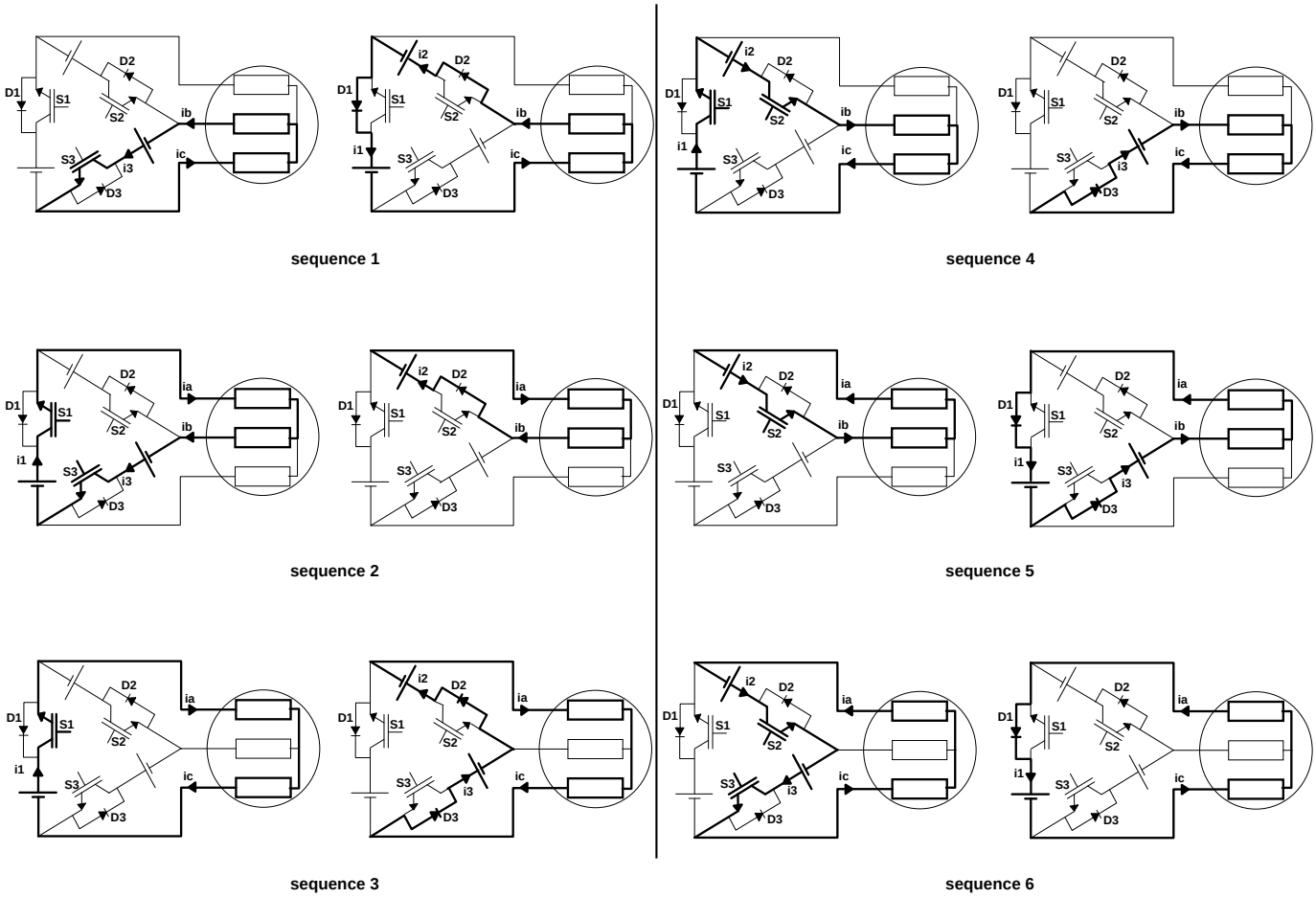

Fig. 2. **T**he six operating sequences of the BLDCM fed by a TSTPI under bang-bang current regulation.**Legend:** (left): active subsequences, (right): regenerative subsequences

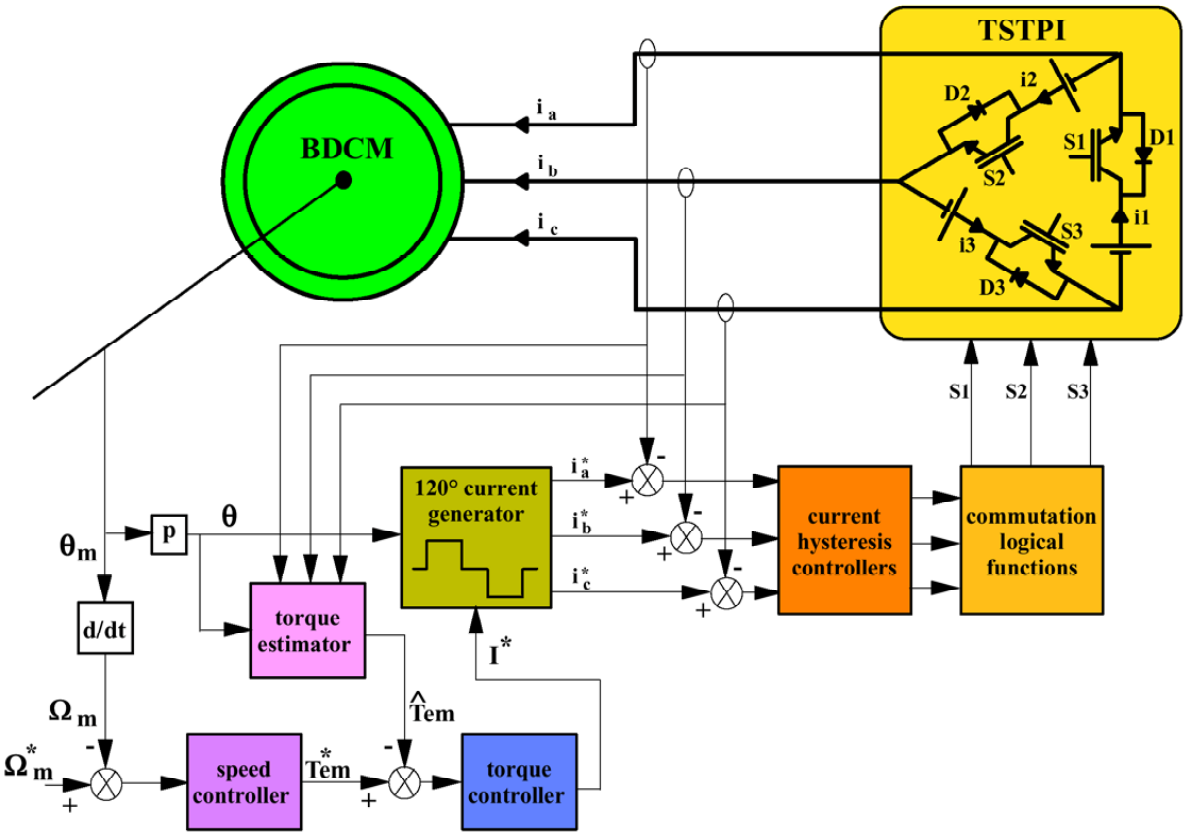

Fig. 3. Block diagram of the control strategy implemented in the TSTPI-fed BLDCM drive

ISBN: 978-988-19252-1-3
ISSN: 2078-0958 (Print); ISSN: 2078-0966 (Online)

TABLE I
CHARACTERIZATION OF OPERATING SEQUENCES OF THE BLDCM. **LEGEND:** SEQ_i^a AND SEQ_i^r INDICATE THE ACTIVE SUBSEQUENCE AND THE REGENERATIVE ONE, RESPECTIVELY, OF SEQUENCE i, WITH $1 \leq i \leq 6$

Sub-sequence	Conducting switch(es)	phase voltages		
		V_a	V_b	V_c
Seq_1^a	S3	e_a	$-\frac{U_{DC}}{6}$	$\frac{U_{DC}}{6}$
Seq_1^r	D1 & D2	e_a	$\frac{U_{DC}}{3}$	$-\frac{U_{DC}}{3}$
Seq_2^a	S1 & S3	$\frac{U_{DC}}{3}$	$-\frac{U_{DC}}{3}$	e_c
Seq_2^r	D2	$-\frac{U_{DC}}{6}$	$\frac{U_{DC}}{6}$	e_c
Seq_3^a	S1	$\frac{U_{DC}}{6}$	e_b	$-\frac{U_{DC}}{6}$
Seq_3^r	D2 & D3	$-\frac{U_{DC}}{3}$	e_b	$\frac{U_{DC}}{3}$
Seq_4^a	S1 & S2	e_a	$\frac{U_{DC}}{3}$	$-\frac{U_{DC}}{3}$
Seq_4^r	D3	e_a	$-\frac{U_{DC}}{6}$	$\frac{U_{DC}}{6}$
Seq_5^a	S2	$-\frac{U_{DC}}{6}$	$\frac{U_{DC}}{6}$	e_c
Seq_5^r	D1 & D3	$\frac{U_{DC}}{3}$	$-\frac{U_{DC}}{3}$	e_c
Seq_6^a	S2 & S3	$-\frac{U_{DC}}{3}$	e_b	$\frac{U_{DC}}{3}$
Seq_6^r	D1	$\frac{U_{DC}}{6}$	e_b	$-\frac{U_{DC}}{6}$

where p is the pole pair number and where Φ_{pm} and I_a are the rms-values of the Permanent Magnet(PM) flux and of the armature current, respectively.

Compared to the control strategy considered in the case of a conventional six-switch three-phase inverter in the armature, the proposed control scheme includes a torque loop, thanks to which, the high torque ripples during sequence-to-sequence commutations have been reduced. These are due to the commutations of the BLDCM power supply from 1/3 to 2/3 (and vice-versa) of the battery pack [11].

Figure 3 shows the block diagram of the proposed control strategy.

The introduction of the torque loop requires the implementation of a torque estimator, which at a first glance would result in a CPU-time consuming procedure. This drawback has been discarded thanks to a simple formulation of the electromagnetic torque based on the normalized back EMF, as follows [11]:

$$T_{em} = K_t \left(f_a i_a + f_b i_b + f_c i_c \right) \tag{2}$$

where K_t is the torque constant, and where $f_{a,b,c}$ and $i_{a,b,c}$ are the a, b, c-phase normalized trapezoidal back EMF and 120°-rectangular current respectively.

Furthermore, unlike conventional inverters, the control of each of the TSTPI IGBTs does not mean the control of the current feeding one of the BLDCM phases. Therefore, the outputs of the current bang-bang controllers could not be directly used to achieve the control of the IGBTs of the delta-inverter. In order to solve this problem, logical functions have been inserted between the outputs of the current controllers and the control inputs of the IGBTs [11].

IV. CONTROL OF MANIPULATOR ARM

Thanks to his control simplicity, the BLDCM is considered as the most suitable actuator for a robot manipulator.

Putting into consideration that a fast and precise movements are necessary to provide to the robot manipulator an excellent dynamic response, it has been shown necessary to require a high dynamic performance of the motor providing in this case a high electromagnetic torque. For this reason, we can not discarded the use of a transmission gearbox system [12].

Similarly, the selection of the control system depend on the characteristics of the motor, as well as the reduction ratio of the gearbox system.

The most common control reported in the literature regarding the association of the robot equipped with a brushless motor and high torque gearbox combination is based on tracking trajectories.

It is based on the generation of the trajectories which describe the evolution in time of each joint. These trajectories must comply with specific constraints such as joint limits of the robot, the feasibility with respect to engine power, etc..

Let us consider, in this work, the case of a robot manipulator with a single degree of freedom.

A. Dynamic Model

Refering to *Lagrange* equation, the dynamic model of an arm can be expressed as follows [13], [14]:

$$A(q)\ddot{q} + C(q,\dot{q})\dot{q} + G(q) = \Gamma \tag{3}$$

with :

- $q = [q_1]^T$ is the angular position,
- $\dot{q} = [\dot{q}_1]^T$ is the angular speed,
- $\ddot{q} = [\ddot{q}_1]^T$ is the angular acceleration,
- A(q) is the positive inertia symmetric matrix,
- $C(q,\dot{q})\dot{q} = B(q)\dot{q}^2 + C(q)\dot{q}\dot{q}$ represent the centrifugal and *Coriolis* forces,
- G(q) represents the couple of gravity,
- $\Gamma = [\Gamma_1]^T$ is the torque applied to the axe of the robot.

The components of $A(q)\ddot{q}$, $C(q,\dot{q})\dot{q}$ and $G(q)$ can be rewritten respectively as follows:

$$A_1 = A_{11}\ddot{q}_1 = (J_1 + m_1 L_{c1}^2)\ddot{q}_1 \tag{4}$$

$$C_1 = 0;\ G_1 = (m_1 L_{c1}) g \cos q_1 \tag{5}$$

It should be noted that *m* is assigned to the masses, *J* for the inertia and *L* for length and the gravity constant g is equal to $9.81\ m.s^{-2}$.

B. Trajectory Generation

The trajectory generation is the part of the control system which imposes setpoints'movement to be followed by moving in a direction towards a final position. Such setpoints can be sent directly to the actuators or to the control loops. Typical instructions of movement contain the definition of displacement , kinematic constraints which the robot must respect such as the execution time, etc.. To do this, it is sufficient to impose an angle of rotation of the load; angle which correspond to a movement along a desired speed requested for an articulated arm.

The problem of path generation lies in the calculation of the setpoint of position, speed and acceleration which are a function of time and which ensure the passage of the robot by a desired path, defined by a sequence of situations of terminal organ or joint configuration. To obtain the desired displacement, we are interested in the expression of the speed depending on time, so that obtaining the desired position at the final instant stops the motor.

ISBN: 978-988-19252-1-3
ISSN: 2078-0958 (Print); ISSN: 2078-0966 (Online)

To control the robot trajectory, we use an encoder associated to the motor.

A control law developing the trajectory of desired speed is described as follows [15] :

$$w_{ref} = 6\,\frac{(\theta_f - \theta_i)\,t}{t_f^2} - 6\,\frac{(\theta_f - \theta_i)\,t^2}{t_f^3} \quad (6)$$

with :

- w_{ref} is the reference speed,
- θ_f is the desired position,
- θ_i is the initial position,
- t_f is the time required to achieve the desired position.,
- t is the time,

C. Decentralized Control of Type PID

When the system presents a linear behavior, the regulation of the movement can be achieved by conventional techniques control. We can note in this case the decentralized control type PID. This technique is widely used by robot manipulators using gear motors with high reduction ratios. Therefore, each joint is controlled by PID control with constant gains due to the facility of its implementation and low cost [16], [17].

Taking into account that, in this work we dispose of an association of a robot arm-brushless DC motor associated with its high reduction ratio, we are interested in the implementation of the control type PID . The PID control law is given by the following relation [16] :

$$\Gamma = K_p(q_d - q) + K_d(\dot{q_d} - \dot{q}) + K_I \int (q_d - q)dt \quad (7)$$

where :

- $\dot{q_d}(t)$ and $q_d(t)$ indicate the references of position and speed in the joint space,
- K_p, K_d and K_I are positive diagonal matrices of dimension (2×2) and they are composed by the proportional K_{pj}, derivative K_{dj} and integral K_{Ij} gains.

The calculation of K_{pj}, K_{dj} and K_{Ij} gains is done by considering the model of the joint "j" represented by the second order linear system as follows:

$$\Gamma_j = A_{jj}(q)\ddot{q_j} + C_j(q,\dot{q})\dot{q_j} + G_j(q) \quad (8)$$

By neglecting $C_j(q,\dot{q})$ et $G_j(q)$, the transfer function of the closed loop system will be given by the following relation:

$$\frac{q_j(s)}{q_{jd}(s)} = \frac{K_{dj}\,s^2 + K_{pj}\,s + K_{Ij}}{A_{jj}\,s^3 + K_{dj}\,s^2 + K_{pj}\,s + K_{Ij}} \quad (9)$$

The characteristic equation is then written:

$$\triangle(s) = A_{jj}\,s^3 + K_{dj}\,s^2 + K_{pj}\,s + K_{Ij} \quad (10)$$

The most common solution in robotics is to choose the gains so as to obtain a real and negative triple pole, which gives the fastest response possible without oscillation.

V. Simulation Results

A. Description of Simulation

The performance of the dedicated self control strategy for TSTPI fed BLDCM have been evaluated through simulation works carried out in the MATLAB-SIMULINK environment. For the sake of comparison, the same control strategy has been also implemented in the case of BLDCM fed by a SSTPI.

Two cases of simulation have been treated:

- the case of the six and three switch three-phase inverter-fed brushless DC motor using an example of a reference speed and reference electromagnetic torque proportional to the speed,
- the case of the six and three switch three-phase inverter-fed brushless DC motor using the angular position, speed and acceleration which are the output of the dynamic model of the robot arm for low speeds.

The main variables that are focused in this analysis are:

- the reference and motor speed (rpm),
- the electromagnetic torque (N.m),
- the phase current i_a, (A),
- the angular position (rad).

We have considered:

- a constant DC voltage of 42V using 14V in each leg in the case of the TSTPI,
- a BLDCM whose ratings are: 42V (DC), 3.4A (DC), 120W and 9290rpm,
- a gear system with: N=74, η=0.72 and Jc=15e-7Kg.m,
- the parameters of the robot arm are: $m_1 = 0.8619Kg$, $L_{c1} = 0.3m$ and $J_1 = 0.0065N.m^2$.

The parameters of the BLDCM used for simulation purpose are tabulated in table II.

TABLE II
Parameters of Brushless Motor

$r_s = 0.29\Omega$	$l_s = 0.29\Omega$	$\phi_r = 0.0473$Wb
$l_{sd} = l_{sq} = 2.7$mH	$p = 2$	$J = 0.05$Kg.m^2

The following drive and control data have been also considered:

- a load torque proportional to the speed:

$$T_l = K_m\Omega_m \quad (11)$$

- a reference speed which takes the shape of a ramp allowing an increase of the speed from 0 to 1500rpm during 1s. This reference speed is only considered for the first case of simulation, where in the second one the reference speed is the output speed of the robot dynamic model.

ISBN: 978-988-19252-1-3
ISSN: 2078-0958 (Print); ISSN: 2078-0966 (Online)

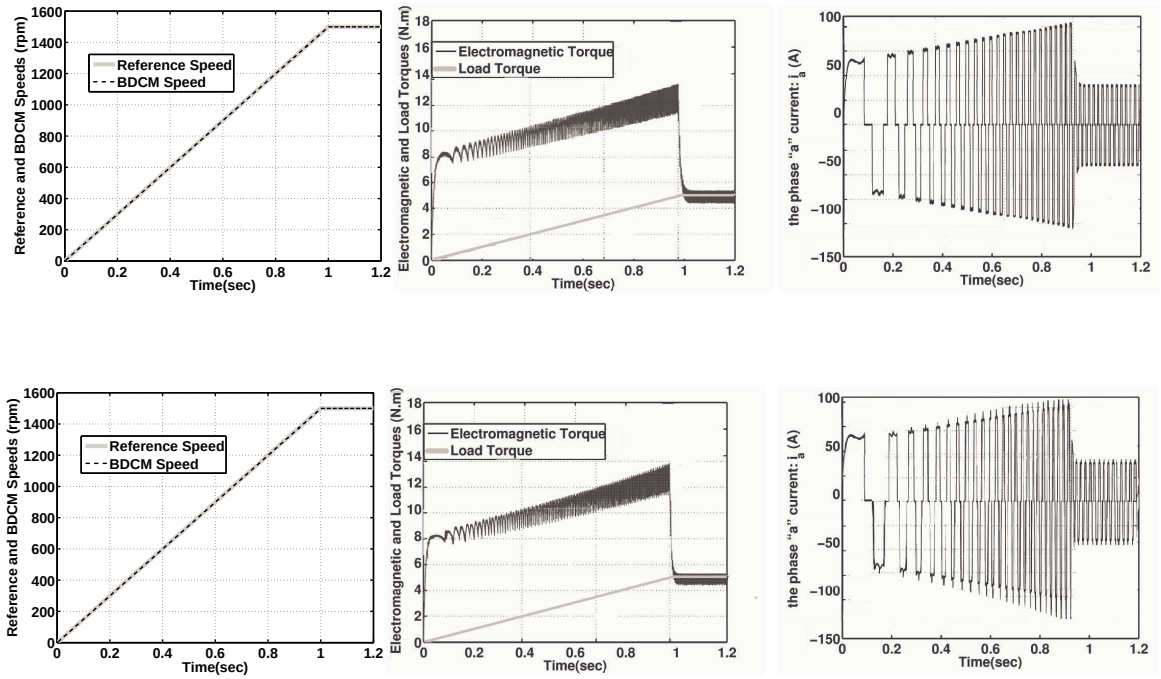

Fig. 4. Transient behavior during the start-up of the BDCM. Legend 1: (left side): the reference speed and the BDCM speed , (middle): the electromagnetic torque and the load torque , (right side): the phase "a" current. Legend 2: up: the case of a SSTPI-fed BDCM drive, down: the case of a TSTPI-fed BDCM drive

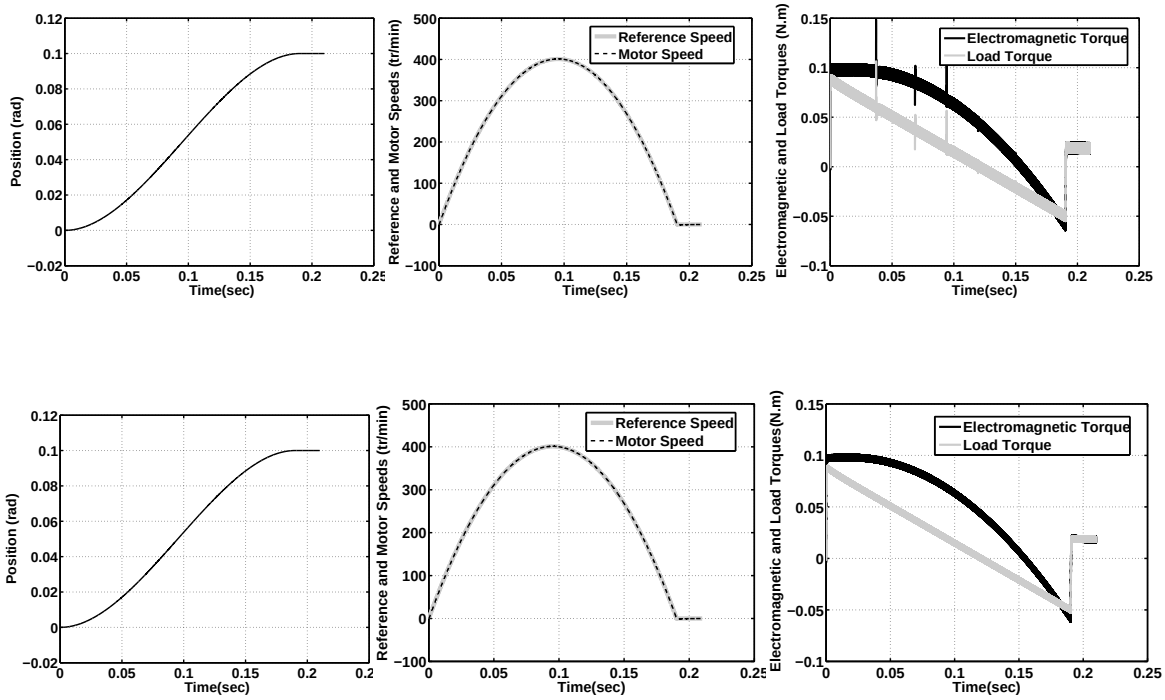

Fig. 5. Transient behavior during the start-up of the BDCM considering a manipulator arm with a single degree of freedom. Legend 1: (left side): Robot angular position, (middle): Reference speed and motor speed, (right side): electromagnetic Torque and Load Torque. Legend 2: up: the case of a SSTPI-fed BDCM drive, down: the case of a TSTPI-fed BDCM drive

ISBN: 978-988-19252-1-3
ISSN: 2078-0958 (Print); ISSN: 2078-0966 (Online)

B. Analysis of Simulation Results

In what follows, simulation results are presented in Figures 4 and 5, where the upper and down figures indicate plots corresponding respectively to the SSTPI and the TSTPI fed BLDCM drive. Following the analysis of Figure 4, it is to be noted that:

- the TSTPI and the SSTPI fed BLDCM drive considering an electromagnetic torque proportional to the speed present almost the same performances during the start-up as well as during the steady state operation,
- the TSTPI fed BLDCM drive is penalized by a torque ripples during sequence to sequence commutation. There are associated with the commutation of the BLDCM power from 1/3 to 2/3 (and vice-versa) of the battery pack. The amplitude of the torque ripple does not effect the performances of the BLDCM,

The simulation results illustrated in Figure 5 show that:

- the manipulator arm with a single degree of freedom follows its desired trajectory with a static error near to zero. This confirms the robustness of the PID controller forcing the joint to converge to a desired position with a definite speed for the two association BLDCM-TSTPI and BLDCM-SSTPI,
- the final desired position is reached if the zero speed is achieved. In this case, the electromagnetic torque is equal to the load torque for both association. As it shown, the behavior of the torque is influenced by the unequal power of the battery pack during the commutation from a sequence to another in the case of the association BLDCM-TSTPI,
- Similar to results found in the association BLDCM-TSTPI developed in the first case of simulation, the rapidity of the CPU-time consuming procedure, is very clear compared to the SSTPI fed BLDCM drive which have a great advantage especially in the robotic application.

Accounting for the reduction of the number of power switches from six to three, the high performance of the TSTPI fed BLDCM motor drives could be regarded as a mature technology for the robotic applications.

VI. Conclusion

This work was developed within the improvement of the reliability, the cost-effectiveness and the compactness of TSTPI fed BLDCM drives to be integrated in robotic systems.

Topologically, a delta-inverter includes three switches rather than six in conventional inverters. Moreover, the BLDCM requires a low-resolution low-cost encoder. These represent crucial cost benefits for robotic applications. The fundamentals of delta-inverter fed BLDCM drives were firstly recalled. A control strategy dedicated to delta inverter fed BLDCM drives was proposed in a second step. A dynamic model and the control of a robot arm have been developed in a third step.

Finally and for the sake of comparison, the same control strategy has been implemented in six-switch three-phase inverter (SSTPI) considering two cases of simulation: (i) the case of a speed reference ramp and (ii) the case where the reference speed is generated from the dynamic model of the robot arm. Simulation results have clearly shown that, like the SSTPI fed BLDCM motor, the implementation of the dedicated control strategy in BLDCM motor fed by a delta-shaped inverter leads to high performance. Giving the 50 per cent structure reduction of the TSTPI compared to SSTPI, this open up crucial benefits from both cost-effectiveness and compactness point of view, especially in the robotic application.

References

[1] L. Bai, “Electric Drive System with BLDC Motor,” *Proc. IEEE International Conference on Electric Information and Control Engineering (ICEICE)*, 2011.

[2] D.S. Sun, X. Cheng and X.Q. Xia,“Research of Novel Modeling and Simulation Approach of Brushless DC Motor Control System,” *Proc. IEEE International Conference on E-Product E-Service and E-Entertainment(ICEEE)*, 2010.

[3] Ji.Hua and Li.Zhiyong “Simulation of Sensorless Permanent Magnetic Brushless DC Motor Control System,” *Proceedings of the IEEE International Conference on Automation and Logistics*,Qingdao, China, September 2008.

[4] B.K. Lee and M. Ehsani, “Advanced BLDC motor drive for low cost and high performance propulsion system in electric and hybrid vehicles,” *IEEE International Electric Machines and Drives Conference (IEMDC’2001)*, Cambridge, Massachusetts, USA, 2001.

[5] N. Hemati, J.S. Thorp and M.C. Leu,“Robust Nonlinear Control of Brushless dc Motors for Direct-Drive Robotic Applications,” *Proc. IEEE Transactions on Industrial Electronics*, vol. 37, no. 6, pp 460-468, March 1990.

[6] J.J. Carroll and D.M. Dawson,“Robust Tracking Control of a Brushless DC Motor with Application to Direct-Drive Robotics,”*Proc. IEEE International Conference on Robotics and Automation*, 1993.

[7] C.Y. Su, Y. Stepanenko and S. Dost ,“Hybrid Integrator Backstepping Control of Robotic Manipulators Driven by Brushless DC Motors,” *in Proc. IEEE/ASME Transactions on Mechatronics*”, vol. 1, no. 4, pp 266 - 277, December 1996.

[8] C.Y. Su and Y. Stepanenko,“Integrator backstepping based hybrid adaptive control of robotic manipulators driven by brushless DC motors,” *Proceedings of the 35th IEEE conference on Decision and Control*, Kobe, Japan, 1996.

[9] H. Melkote and F. Khorrami, “Robust Adaptive Control of Direct Drive Brushless DC Motors and Applications to Robotic Manipulators,” *Proceedings of the 1997 IEEE International Conference on Control Applications*, Hartford, CT, October 5-7, 1997 .

[10] H. Melkote and F. Khorrami, “Nonlinear Adaptive Control of Direct-Drive Brushless DC Motors and Applications to Robotic Manipulators,” *IEEE/ASME Transactions on Mechatronics*, vol. 4, no. 1, pp 71-81, March 1999.

[11] A. Elantably, A. Ben Rhouma, A. Masmoudi and A.G. Holmes, “Control device for driving a brushless DC motor,” *US Patent 7643733*, 2010.

[12] G. Grillet and G. Clerc, “Electrical actuators, principles, models, control,” *Editions Eyrolles*, Paris, France, 1997.

[13] N. Mezghani Ben Romdhane, T. Damak, “Terminal sliding mode feedback linearization control,” *International Journal of Sciences and Techniques of Automatic control and computer engineering*, vol. 4, no. 1, pp 1174-1187, July 2010.

[14] V. Padois, “Control of Robotic Systems,” *Note of master courses, Institute of Intelligent Systems and Robotics*, Pierre and Marie Curie University, 2010.

[15] M. Pinard, “Electronic control of electrical motors,” *Editions DUNOD*, 2007.

[16] L. Adouane, “Modelisation and control of robots,” *Note of course for Electrical Engineer: Polytech Clermont Ferand*, 2010.

[17] K. Khial, “Position control of a Servo System Including a Harmonic Gear with torque measurement and compensation of Non-Linearity,” *Project Graduation* in Applied Sciences, Polytechnic school of Montreal. Department of Electrical Engineering and Computer Engineering Automation Section, 2001.

ISBN: 978-988-19252-1-3
ISSN: 2078-0958 (Print); ISSN: 2078-0966 (Online)